REPORT DOCUMENTATION PAGE

Form Approved OMB No. 0704-0188

1. AGENCY USE ONLY (Leave blank)	2. REPORT DATE	3. REPORT TYPE AND DATES COVERED
	November 1993	Final Report

4. TITLE AND SUBTITLE

Prediction of Atmospheric MTF and Application to Image Restoration, Based on Meteorological Data.
First Quarterly Report

5. FUNDING NUMBERS

F6170893W0896

6. AUTHOR(S)

I. Dror and N.S. Kopeika

7. PERFORMING ORGANIZATION NAME(S) AND ADDRESS(ES)

Ben Gurion University of the Negev
Department of Electrical and Computer Engineering
Beer Sheva, Israel 84105

8. PERFORMING ORGANIZATION REPORT NUMBER

SPC-93-40603

9. SPONSORING/MONITORING AGENCY NAME(S) AND ADDRESS(ES)

EOARD
PSC 802 BOX 14
FPO 09499-0200

10. SPONSORING/MONITORING AGENCY REPORT NUMBER

SPC-93-4060

11. SUPPLEMENTARY NOTES

19980501 177

12a. DISTRIBUTION/AVAILABILITY STATEMENT

Approved for public release; distribution is unlimited.

12b. DISTRIBUTION CODE

A

13. ABSTRACT (Maximum 200 words)

Predictions of atmospheric transmittance in desert aerosol environments using MODTRAN code diverge significantly from measured data. Good prediction of the desert particulate size distribution is required in order to predict atmospheric scattering and absorption parameters. It is also essential to the prediction of the aerosol atmospheric modulation transfer function which is often the dominant component of the overall atmospheric MTF. Recently an effort to predict statistics but not size distribution according to simple weather parameters has been made for coarse desert aerosols. A quantitative analysis of the desert particulate size distribution models was also performed. In this research, the size distribution parameters measured by optical counters are related to weather parameters. Known statistical and analytical models such as MODTRAN relate the size distribution parameters only to relative humidity for continental atmospheres. Although humidity has a significant role in the prediction of aerosol size statistics, other weather parameters are seen here to strongly influence also the size distribution parameters. Comparisons such as the above can be used to predict under which conditions the MODTRAN aerosol models have good or poor accuracy. It is also hoped that they will lead to improvements in MODTRAN, improving the accuracy of the humidity dependence as well as by incorporating other meteorological parameters into the MODTRAN prediction models.

14. SUBJECT TERMS	15. NUMBER OF PAGES
	16. PRICE CODE

17. SECURITY CLASSIFICATION OF REPORT	18. SECURITY CLASSIFICATION OF THIS PAGE	19. SECURITY CLASSIFICATION OF ABSTRACT	20. LIMITATION OF ABSTRACT
UNCLASSIFIED	UNCLASSIFIED	UNCLASSIFIED	UL

PREDICTION OF ATMOSPHERIC MTF AND APPLICATION TO IMAGE RESTORATION, BASED ON METEOROLOGICAL DATA

First Quarterly Report

(November 1993)

N. S. Kopeika, Principal Investigator

Department of Electrical and Computer Engineering

Ben-Gurion University of the Negev

Beer-Sheva, Israel

original image restorations

Prediction of Atmophseric MTF and

Application to Image Restoration, Based on Meteorological Data:

First Quarterly Report

This quarter work has been concentrated on image restoration techniques based upon atmospheric modulation transfer function (MTF), as well as ordering equipment and getting organized.

The image restoration work is intended for near infrared wavelengths according to the laser radar wavelength (1.06μm) at Eglin AFB. At such wavelengths image degradation by the atmosphere derives from both turbulence and aerosol forward scatter. The former is dominant usually around mid-day while the latter is usually dominant the rest of the time.

A novel image restoration technique has been developed here which utilizes a Weiner filter optimized for turbulence effects, which are often strongly time-varying. This technique corrects also for aerosol-derived blur, unlike adaptive optics techniques which correct only for time-varying tilt (turbulence). The technique is described in the enclosed appendix. It is very quick and, with modern parallel-processing transputers, is capable of producing restored images in a fraction of a second. This new technique is based upon knowledge of average MTF. In the experiments here, average atmospheric MTF was measured.

Efforts in the next few quarters are to be concentrated upon prediction of atmospheric MTF according to weather, thus permitting image restoration according to weather. A technique for predicting turbulence MTF has already been developed. Hence, efforts are to be concentrated upon prediction of aerosol MTF. To this end, a pc version of Modtran (USAF Geophysics Lab) has been purchased so as to enable us to work with marine atmospheres when winds at Eglin are from the south. The MODTRAN/LOWTRAN marine models are known to be fairly reliable. We are developing our own models to predict aerosol size distribution and MTF for continental atmospheres. These are to be compared to Modtran predictions and to experimental measurements.

Transmission predictions are to derive from aerosol size distribution predictions, as well as aerosol MTF predictions.

APPENDIX

High resolution restoration of images distorted by the atmosphere, based upon average atmospheric MTF

D. Sadot, A. Rosenfeld, G. Shuker, and N. S. Kopeika

Department of Electrical and Computer Engineering

Ben-Gurion University of the Negev

Beer-Sheva, Israel

Abstract

A new method of real-time high resolution imaging through the atmosphere is presented. This technique is based on the knowledge of average atmospheric MTF at the time the image is received. Atmospheric effects are modeled by a noisy spatial frequency filter including an average component described by the average atmospheric modulation transfer function, and a noisy component modeled by the atmospheric point spread function's power spectral density. Analytical results are accompanied by experimental image restoration examples, indicating significant image quality improvement based upon knowledge of average atmospheric MTF. This method can be used to help overcome the jitter characteristics of turbulence, and is capable of yielding real-time image restoration with resolution limited essentially only by the hardware itself.

1. Introduction

Imaging through the atmosphere has progressed significantly in the last decade, in both the visible and infrared spectral ranges. It is the atmosphere which usually limits image quality, particularly for long atmospheric paths. The main atmospheric distortions are caused by optical turbulence, and scattering and absorption by particulates in the atmosphere. The main effect of the turbulent medium over long exposures is to produce wavefront tilt, which causes image shifts at the image plane. These can be whole image shifts, or different shifts of different parts of the image, depending on the isoplanatic patch, according to the turbulence parameters (turbulence strength, inner and outer scales). The image distortions caused by the wavefront tilt (typically on the order of tens or maybe hundreds of microradians) can be partially compensated for either by adaptive optics techniques or by using sufficiently short exposure time, less than the characteristic fluctuation time (usually a few milliseconds). Another way is by using a wavefront sensor to construct the image phase in addition to image intensity, and therefore restore the image in a deterministic way[1]. This is however not practical for real time restoration. Turbulence distortion effects are characterized in both short and long exposures by modulation transfer functions (MTFs)[2,3]. These are statistical averages of turbulence random processes which have, in addition, a nonnegligible short-time variance which affects significantly image blur. In addition to turbulence, there are scattering and absorption effects produced by molecules and aerosols in the atmosphere. These cause both attenuation and image blur, according to the atmospheric aerosol MTF[4-7]. Unlike turbulence, the aerosol MTF affecting the image is also related strongly to instrumentation limitations[6,7] on angles of light scatter actually recorded in the image. Thus, aerosol effects can be approximated by an MTF of limited long-time variation, according to weather conditions.

2. Theory

Here, a new method is developed for restoration of images distorted by the atmosphere, based on prior knowledge of both average turbulence and aerosol MTFs. The atmosphere is modeled as a random filter

$$h' = h + n_1 \tag{1}$$

where h' is the instantenous atmospheric point spread function (PSF), h is the average atmospheric PSF, and n_1 is an additive random component with zero expectation. Using this model, the image received at the imaging system after propagating through the atmosphere is:

$$g(x,y) = \left(h(x,y) + n_1(x,y)\right) \otimes f(x,y) + n_2(x,y) \tag{2}$$

where g is the received image, f is the object, x and y are transverse spatial coordinates, and n_2 is an additive noise imposed by the instrumentation, including optics, digitization, electronics etc., but not by the atmosphere. Fourier transforming (2) yields:

$$G(u,v) = [H(u,v) + N_1(u,v)] \cdot F(u,v) + N_2(u,v) \tag{3}$$

where G, H, F, N_1 and N_2 are Fourier transforms of g, h, f, n_1 and n_2 respectively, and u and v are spatial frequency coordinates. The received image thus is a sum of a deterministic part G_1 and a random part N

$$G = G_1 + N \tag{4}$$

where

$$G_1(u,v) = H(u,v) \cdot F(u,v) \tag{4.a}$$

and

$$N(u,v) = F(u,v) \cdot N_1(u,v) + N_2(u,v). \tag{4.b}$$

The optimal image restoration filter in terms of maximal signal to noise ratio (SNR) is the Wiener filter[8,9]

$$M(u,v) = \frac{|H(u,v)^2|}{H(u,v) \cdot \left(|H(u,v)^2| + \left[S_{nn}(u,v) / S_{ff}(u,v)\right]\right)} \tag{5}$$

where M is the restoring filter, S_{nn} and S_{ff} are the power spectral densities (PSDs) of f and n, n being the inverse Fourier transform of N. Substituting (4.b) into (5) and assuming statistical independence between f, n_1, and n_2, yields

$$M(u,v)=\frac{|H(u,v)^2|}{H(u,v)\cdot\left(|H(u,v)^2|+\left[S_{n1n1}+S_{n2n2}(u,v)/S_{ff}(u,v)\right]\right)}. \tag{6}$$

The restored image intended to represent the original object is then evaluated by multiplying the filter by the received image spectrum in the frequency domain:

$$\hat{F}(u,v)=\frac{G(u,v)}{H(u,v)}\cdot\frac{|H(u,v)^2|}{|H(u,v)^2|+\left[S_{n1n1}+S_{n2n2}(u,v)/S_{ff}(u,v)\right]}. \tag{7}$$

In order to use (7), all its terms must be either calculated or estimated. The term $H(u,v)$ is the average atmospheric modulation transfer function (MTF). Assuming independence between aerosol and turbulence effects, this term can be measured or calculated by a multiplication of the turbulence MTF (either short or long exposure case) and aerosol MTF. Turbulence MTF can be evaluated with the knowledge of standard meteorological parameters using a C_n^2 prediction model[10] (verified independently by U.S. Army Night Vision Laboratory) or IMTURB or PROTURB, and the aerosol MTF[6] can be evaluated according to knowledge of particle size distribution, which can also be predicted via LOWTRAN, MODTRAN, or other models[11]. The term $S_{ff}(u,v)$ can be estimated either by using the received image $G(u,v)$ or by using estimation models of the object's PSD, which has been shown to obey a fractal model in the visible range, and a Markovian model in the thermal range[12]. The term $S_{n_2n_2}(u,v)$ is assumed to be constant for all spatial frequencies since the additive noise n_2 is assumed to be white noise. This assumption is commonly used and very practical, and it has a relatively weak effect on the Wiener filter. The term $S_{n_1n_1}(u,v)$ is very important, since it includes the random part of the atmospheric distortions. If this term can be evaluated, then a Wiener filter can be used for restoration of images distorted by the atmosphere.

One way of estimating $S_{n_1n_1}(u,v)$ is by a direct measurement. By using the relation

$$S_{n_1n_1}=E\{N_1^2\}=E\{H'^2\}-H^2 \tag{8}$$

where H' is the Fourier transform of h', the variance of H' can be evaluated by calculating both terms of the right hand side of (8). This can be carried out by measuring a series of instantaneous atmospheric MTFs, and evaluating the average of both the MTF and its square. This is, however, not a very practical way, particularly when *real time* image restoration is

concerned. It should be pointed out that the contribution to the random part of the atmospheric MTF is due mainly to turbulence rather than aerosols. Therefore, in the rest of the discussion, particularly in eqs. (8)-(19), for all practical purposes atmospheric MTF and PSF refer to turbulence only since aerosol MTF displays much less jitter. However, in eqs. (6)-(7) $H(u,v)$ includes aerosol MTF in addition to turbulence MTF since it refers to average atmospheric MTF.

Here, an analytical way is presented of calculating $S_{n_1n_1}(u,v)$ by evaluating both terms of the right hand side of (8). The second term H^2 is the square of the turbulence MTF which can be predicted[10] or measured. The first term $E\{H'^2\}$ is to be evaluated here analytically.

The instantaneous MTF of turbulence is given by[3]

$$H'(u,v) = \frac{\iint \exp\{\chi(x,y)+\chi(x-\lambda fu, y-\lambda fv)\}dxdy}{\iint \exp\{2\chi(x,y)\}dxdy} \tag{9}$$

where $\chi = \ln\frac{A}{A_0}$ is the wave log amplitude fluctuation, A is the wave amplitude and A_0 is the wave amplitude in the absence of turbulence, f is the imaging system's focal plane, and λ is the radiation wavelength. In a similar way, H'^2 is given by

$$H'^2(u,v) = \frac{\iint\iint \exp[\chi(x,y)+\chi(x-\lambda fu, y-\lambda fv)+\chi(x-\Delta x, y-\Delta y)+}{\iint\iint \exp[2\chi(x,y)+2\chi(x-\Delta x, y-\Delta y)]dxdyd\Delta xd\Delta y}$$
$$\frac{+\chi(x-\Delta x-\lambda fu, y-\Delta y-\lambda fv)]dxdyd\Delta xd\Delta y}{\iint\iint \exp[2\chi(x,y)+2\chi(x-\Delta x, y-\Delta y)]dxdyd\Delta xd\Delta y}. \tag{10}$$

Under the assumption of ergodicy, the ensemble average MTF will be identical with the long exposure MTF, and if we assume that the spatial statistics of the medium are Wide Sense Stationary (WSS), the expected values are independent of x and y and can be factored outside the integrals. The denominator in (10) is a normalizing factor which is the zero frequency value, and will be ignored for the rest of this analysis for simplicity. The result is an average of the square of the optical transfer function given by

$$E\{H'^2(u,v)\} = \iint E\{\exp[\chi(x,y)+\chi(x-\lambda fu, y-\lambda fv)+ \\ +\chi(x-\Delta x, y-\Delta y)+\chi(x-\Delta x-\lambda fu, y-\Delta y-\lambda fv)]\} d\Delta x d\Delta y. \tag{11}$$

To aid in this calculation, we use the relations[3]

$$E\{\exp(z)\} = \exp(E\{z\}+\tfrac{1}{2}\mathrm{var}\{z\}) \tag{12}$$

where z is any Gaussian random variable (as χ is), and

$$E\{\chi\} = -c_\chi(0) \tag{13}$$

where c is the covariance function. The expectation and variance of the variable at the exponent are:

$$E\{\chi(x,y)+\chi(x-\lambda fu, y-\lambda fv)+\chi(x-\Delta x, y-\Delta y)+ \\ +\chi(x-\Delta x-\lambda fu, y-\Delta y-\lambda fv)\} = 4\overline{\chi} = -\,4c_\chi(0) \tag{14}$$

$$\begin{aligned}
&\tfrac{1}{2}\mathrm{var}\{\chi(x,y)+\chi(x-\lambda fu, y-\lambda fv)+\chi(x-\Delta x, y-\Delta y) \\
&+\chi(x-\Delta x-\lambda fu, y-\Delta y-\lambda fv)\} = \\
&=\tfrac{1}{2}E\left\{\begin{bmatrix}(\chi(x,y)-\overline{\chi})+(\chi(x-\lambda fu, y-\lambda fv)-\overline{\chi})+ \\ +(\chi(x-\Delta x, y-\Delta y)-\overline{\chi})+ \\ +(\chi(x-\Delta x-\lambda fu, y-\Delta y-\lambda fv)-\overline{\chi})\end{bmatrix}^2\right\} = \\
&= 2c_\chi(0)+2c_\chi(\lambda fu,\lambda fv)+2c_\chi(\Delta x,\Delta y)+c_\chi(\Delta x+\lambda fu,\Delta y+\lambda fv)+ \\
&+c_\chi(\Delta x-\lambda fu,\Delta y-\lambda fv).
\end{aligned} \tag{15}$$

Substituting (14) and (15) into (12), and than into (11) yields:

$$\begin{aligned}
&E\{H'^2(u,v)\} \propto \iint \exp[-\,2c_\chi(0)+2c_\chi(\lambda fu,\lambda fv)+2c_\chi(\Delta x,\Delta y)+ \\
&+c_\chi(\Delta x+\lambda fu,\Delta y+\lambda fv)++c_\chi(\Delta x-\lambda fu,\Delta y-\lambda fv)]d\Delta x d\Delta y = \\
&=\exp[4c_\chi(0)]\iint \exp[-\,6c_\chi(0)+2c_\chi(\lambda fu,\lambda fv)+2c_\chi(\Delta x,\Delta y)+ \\
&+c_\chi(\Delta x+\lambda fu,\Delta y+\lambda fv)+c_\chi(\Delta x-\lambda fu,\Delta y-\lambda fv)]d\Delta x d\Delta y.
\end{aligned} \tag{16}$$

Using the relation between the turbulence MTF and the covariance function[3]

$$H(u,v) \propto \exp(-c_\chi(0)+c_\chi(\lambda fu,\lambda fv)) \tag{17}$$

and the change of variables:

$$u' = \frac{\Delta x}{\lambda f} \qquad v' = \frac{\Delta y}{\lambda f} \tag{18}$$

Eq. (16) can be simplified to yield:

$$E\left\{H'^2(u,v)\right\} \propto H^2(u,v) \iint_{\infty} H^2(u',v')H(u'+u,v'+v)H(u'-u,v'-v)du'dv'. \tag{19}$$

Equation (19) determines the expected value of the squared MTF, or in other words the Point Spread Function's Power Spectral Density, and is the final result of this analysis. This evaluation permits Wiener filter restoration.

The advantage of this result is that for this restoration technique the only information needed to evaluate (19) is the atmospheric average MTF. One has to measure or estimate the average turbulence MTF, then substitute it in (19) and (8) to yield $S_{n_1n_1}(u,v)$, and apply it to (7). As mentioned above, the value $S_{n_1n_1}(u,v)$ was evaluated only by considering turbulence and not aerosol effects. This is not the case at all when dealing with the average value of the atmospheric MTF in (7). Aerosols are not negligible at all in deriving the overall atmospheric MTF, and sometimes are even the dominant part of it[13]. Thus, aerosol MTF must be included in $H(u,v)$ in (7).

3. Experiment

A set of experiments was carried out in the open atmosphere in order to examine this method. An imaging system, including a Pulnix ccd camera model TM-765, connected to a Questar telescope of 1600 mm effective focal length, was located inside the remote sensing laboratory of the electrical and Computer Engineering. Dept. Visible images were recorded over a horizontal pathlength of 6.5 km, with an average path elevation of 25 meters. No wavelength filters were used. Simultaneously, atmospheric MTF was measured via PSF measurements. This was carried out using a 4 mW HeNe laser at 0.6328 μm wavelength, located adjacent to the objects in the object plane. At 6.5 km distance, the laser aperture (< 1

cm) served as a point source. The output signal from the ccd camera was digitized by a Data-Translation frame grabber and sent to a 486 personal computer for further analysis. Fourier transform of the PSF yielded the product of the imaging system and atmospheric MTFs. Division by measured system MTF (Fig. 1) yielded atmospheric MTF.

4. Results

Typical measured average and standard deviation atmospheric MTF for a set of 100 images of the laser aperture are presented in Fig. 2. Fig. 3 presents the average squared *measured* atmospheric MTF for this set. In Fig. 4, the *calculated* average squared atmospheric MTF is presented, using (19). The ratio between the measured and calculated squared atmospheric MTF is presented in Fig. 5. It can be recognized that an excellent agreement is achieved between theory and measurement, except at very high spatial frequencies. This can be explained by small inaccuracies in the measurement of atmospheric MTF at the very high frequencies, where the system's MTF is very poor and the MTF measurement is more likely to be affected by noise. Division by such low MTF values implies large imaging errors in atmospheric MTF even for small errors in imaging system MTF.

Examples of restored images using this new technique are presented in Figs. 6 and 7. The restoration was carried out by using (7). The term $H(u,v)$ used was the measured atmospheric MTF. The term $S_{ff}(u,v)$ was estimated by best fit to a fractal model[12]. The term $S_{n_2n_2}(u,v)$ was assumed to be white noise and the term $S_{n_1n_1}(u,v)$ was evaluated via (19). Restoration time was only about 2 seconds per frame. This can be shortened to a fraction of a second, using parallel processing techniques already available. Therefore restoration via this method can be in real time. There is a distinct improvement in fine details of the images, even though the image's SNR is not degraded significantly. This is so in spite of the severe imaging conditions (long horizontal distance), where turbulence isoplanatic patch was much less than image size, and standard Wiener filters failed completely in trying to restore the image, as can be seen in Fig. 8 where a Wiener filter characterized by (5) has been used. In this case

$S_{nn}(u,v)$ refers to white noise only. On the other hand, in the restored images of Figs. 6 and 7, it is generally quite possible to see detail at 6.5 km almost as small as limited by instrumentation, i.e., $\Delta x = \frac{1}{2u_{\max}} \approx 7\text{cm}$ where $u_{\max}$ is system bandwidth ($\approx$ 50 cycles·mrad^{-1} from Fig. 1). Examples are poles in a fence in Fig. 6 and antenna bars in Fig. 7. This means that, essentially, most of atmospheric blur is removed in the restoration process, and the distant object scene is observed as if there were no atmosphere. Such restoration based on atmospheric MTF does not depend on target shape. It is a fundamental image correction, which can be followed by other image processing techniques as desired. There are cases where turbulence is not so severe, and aerosol MTF plays the most important role in determining the atmospheric MTF, such as in the case of thermal imaging[14], and the image restoration task is much easier[7] since the atmospheric MTF then is nearly deterministic. Here, however, the correction is for both aerosol and turbulence derived blur.

Although the experiment here is based upon measured atmospheric MTF via PSF, in principle it can be applied too to predicted atmospheric MTF.[7,10,11]

5. Conclusions

Restoration of visible images distorted by the atmosphere is presented based upon atmospheric MTF. Such restoration is fundamental and yields image quality limited essentially by instrumentation, as if there were no atmosphere. The atmosphere is modeled by a noisy spatial frequency filter including an average component described by the MTF, and a noisy component modeled by the PSF's power spectral density. An analytical method of deriving the turbulence PSF's power spectral density is developed. This is used to optimize Wiener filter signal-to-noise ratio. It seems that when dealing with high resolution visible and near infrared imaging through long distances, atmospheric distortions need no longer be treated as a deterministic filter represented by average MTF, but can now be modeled as an inherent part of the noise in the received image. Determining this random part is essential to achieve improved

restored images, and a method of doing so is presented here. This method can be used to help overcome the jitter characteristic of turbulence, and is capable of real time image restoration via parallel processing transputers.

Acknowledgment

This work is supported partially by the U.S. Air Force under contract F6170893w0896.

References

1. J. Primot, G. Rousset and J. C. Fontanella, Deconvolution from wavefront sensing: a new technique for compensating turbulence-degraded image," *J. Opt. Soc. of Amer. A,* **7**, No. 9, pp. 1598-1608, September 1990.
2. D. Fried "Optical resolution through a randomly inhomogeneous medium for very long and very short exposure," *J. Opt. Soc. of Amer.* **56**, No. 10, 1372-1379, October 1966.
3. J. W. Goodman, *Statistical Optics*, John Wiley & sons, New York, 1985.
4. A. Ishimaru, *Wave propagation and scattering in random media,* Volume 1, Academic Press, New York, 1978.
5. R. F. Lutomirski "Atmospheric degradation of electrooptical system performance," *Applied Optics*, **17**, No. 24, pp. 3915-3921, December, 1978.
6. D. Sadot and N. S. Kopeika, "Practical instrumentation-based theory and verification of aerosol MTF," *J. Opt. Soc. of Amer. A,* **10**, No. 1, pp. 172-179, January 1993.
7. D. Sadot, A. Dvir, I. Bergel and N. S. Kopeika, "Restoration of thermal images distorted by the atmosphere, based upon measured and theoretical atmospheric modulation transfer function," to be published in *Optical Engineering*, **33**, January 1994 (special issue on Infrared Technology).
8. L. Guan and R. K. Ward, "Restoration of randomly blurred images by the Wiener filter," IEEE, *Trans. on Acoustics, Speech, and Signal Processing*, **12**, No. 4, pp. 589-592, April 1989.

9. A. Rosenfeld, and A. C. Kak, *Digital picture processing*, Academic Press, London, 1976.

10. D. Sadot and N. S. Kopeika, "Forecasting optical turbulence strength on the basis of macroscale meteorology and aerosols: models and validation," *Optical Engineering* **31**, No. 2, pp. 202-212, February, 1991.

11. I. Dror and N. S. Kopeika, "Prediction of particulate size distribution according to weather parameters," in *Atmospheric Propagation and Remote Sensing*, A. Khonle and W. B. Miller eds., Proc. SPIE, Vol. 1668, pp. 123-131, 1992.

12. G. Tidhar, S. R. Rotman, and M. L. Kowalczyk," Clutter matrics for target detection systems," IEEE Trans. on Aerospace and Electr. Syst., Jan 1994 (in press).

13. I. Dror and N. S. Kopeika, "aerosol and turbulence MTFs: comparison measurements in the open atmosphere," Opt. Lett. **17**, No. 22, pp. 1532-1534, 15 Nov. 1992.

14. D. Sadot and N. S. Kopeika "Thermal imaging through the atmosphere: Atmospheric MTF theory and verification," to be published in *Optical Engineering,* **33**, March 1994.

Figure Captions

Fig. 1. Measured imaging system MTF.

Fig. 2. Measured average atmospheric MTF with standard deviation.

Fig. 3. Measured atmospheric PSF's power spectral density.

Fig. 4. Calculated atmospheric PSF's power spectral density.

Fig. 5. Division of measured atmospheric PSF's power spectral density by calculated atmospheric PSF's power spectral density.

Fig. 6. Comparison between original and restored atmospherically distorted images for 6.5 km distance.

Fig. 7. Same as in Fig. 5, but for a different scene at same distance.

Fig. 8. Image restoration using standard Wiener filter.

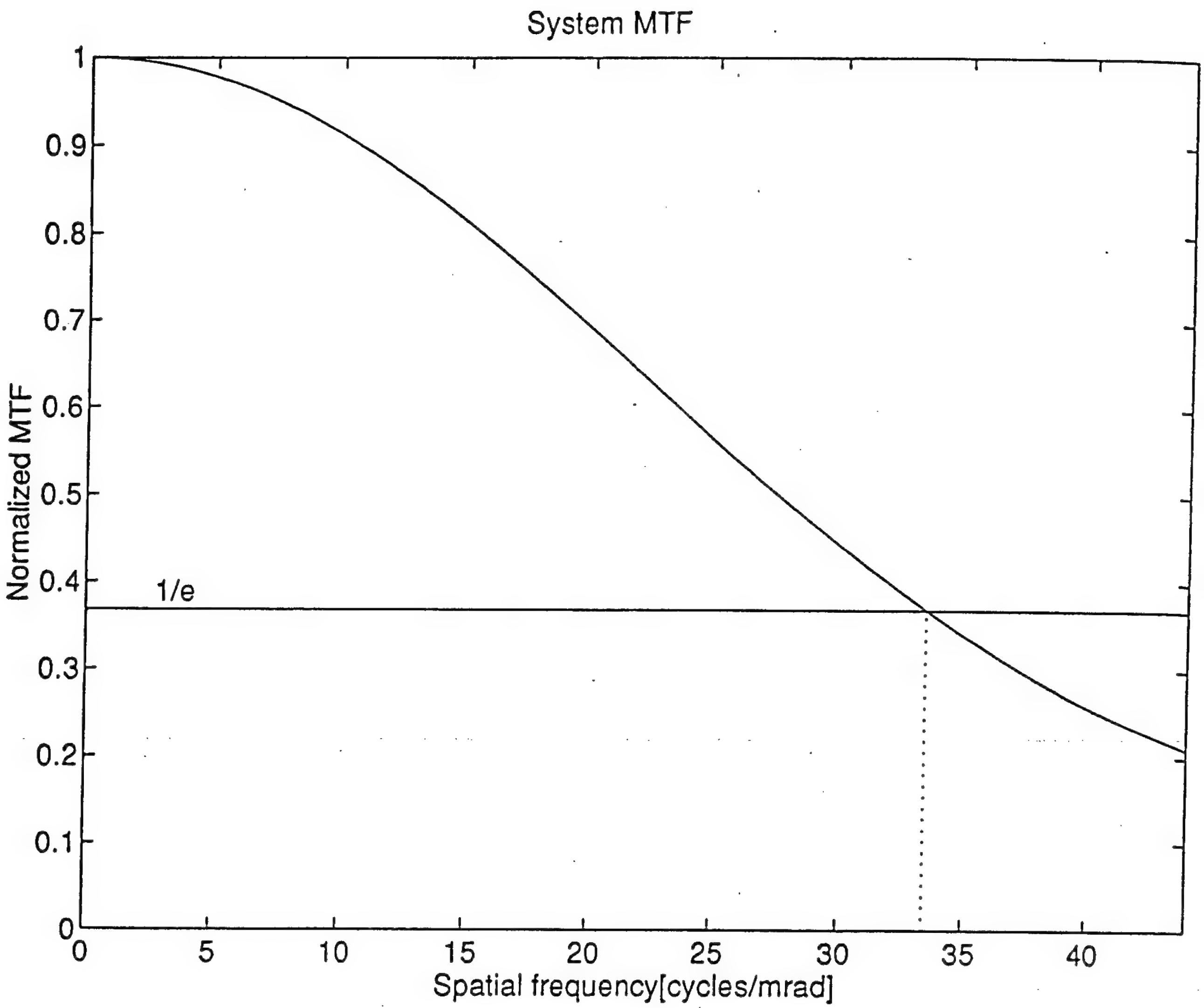
System MTF
Normalized MTF
Spatial frequency[cycles/mrad]
1/e
0
0.1
0.2
0.3
0.4
0.5
0.6
0.7
0.8
0.9
1
0
5
10
15
20
25
30
35
40

Fig 1

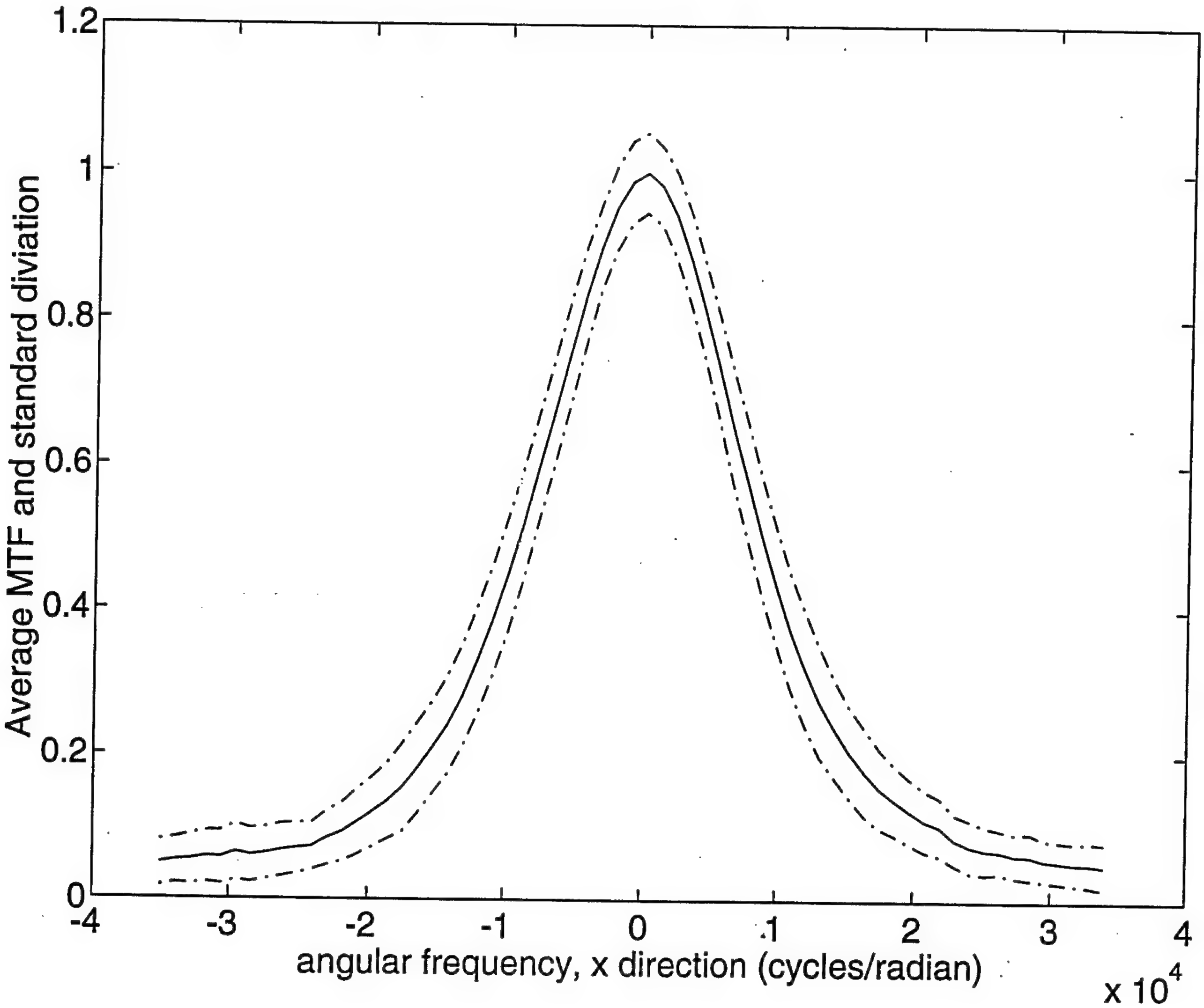
1.2
1
0.8
0.6
0.4
0.2
0
-4
-3
-2
-1
0
1
2
3
4
Average MTF and standard diviation
angular frequency, x direction (cycles/radian)
x 10^4

Fig 2

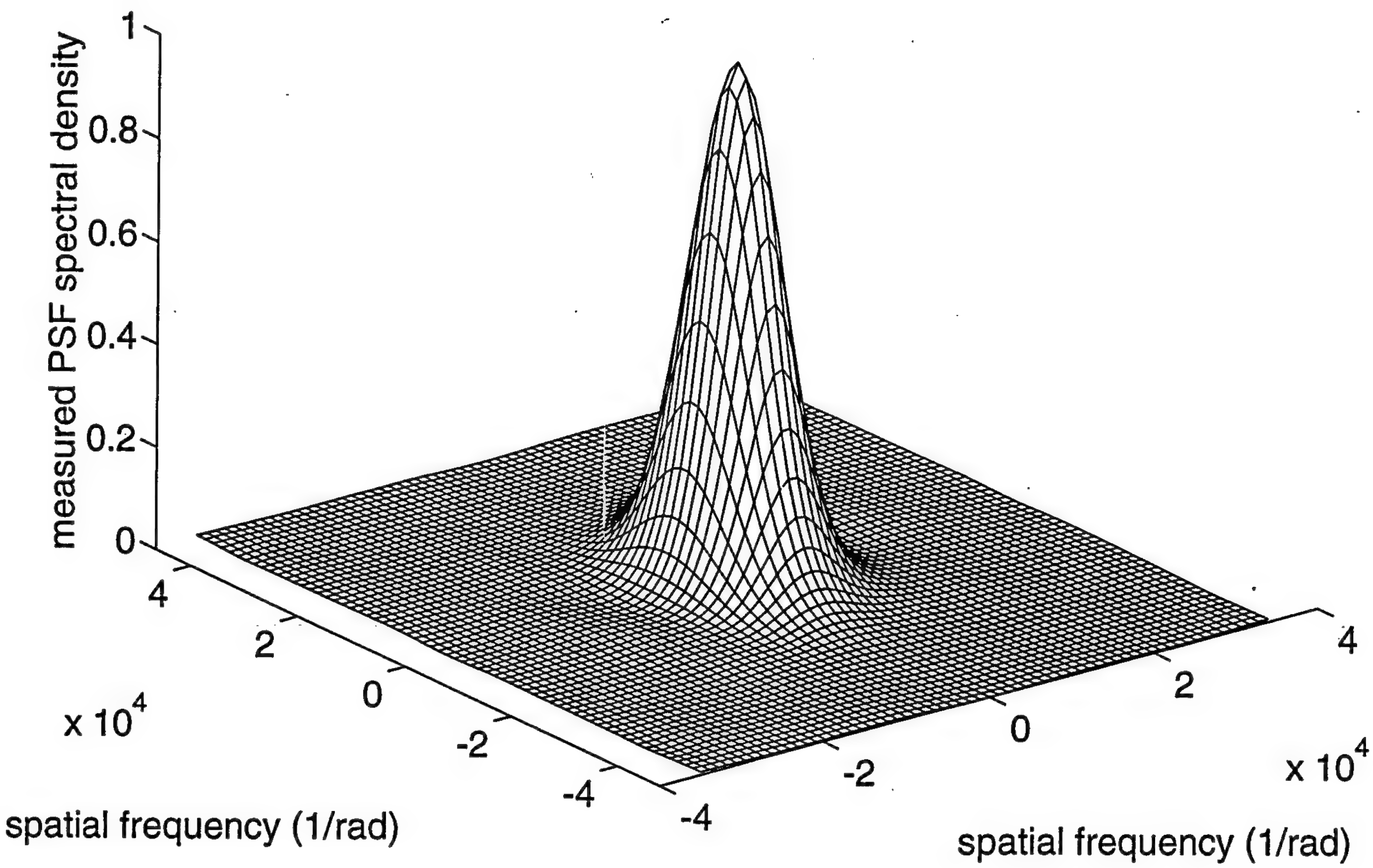

measured PSF spectral density
1
0.8
0.6
0.4
0.2
0
4
2
0
-2
-4
x 10^4
spatial frequency (1/rad)
4
2
0
-2
-4
x 10^4
spatial frequency (1/rad)

Fig 3

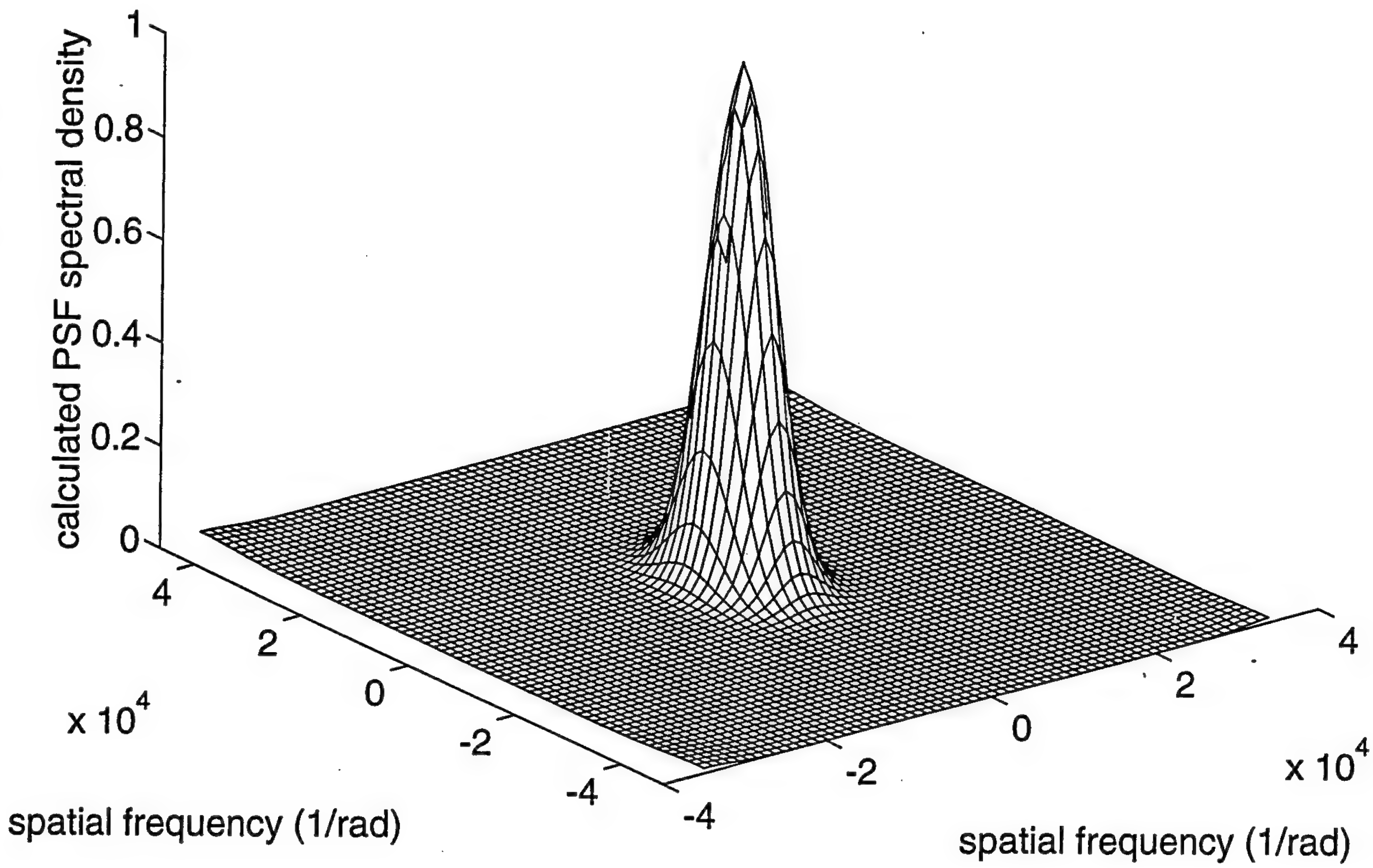
1
0.8
0.6
0.4
0.2
0
calculated PSF spectral density
4
2
0
-2
-4
x 10^4
spatial frequency (1/rad)
-4
-2
0
2
4
x 10^4
spatial frequency (1/rad)

Fig 4

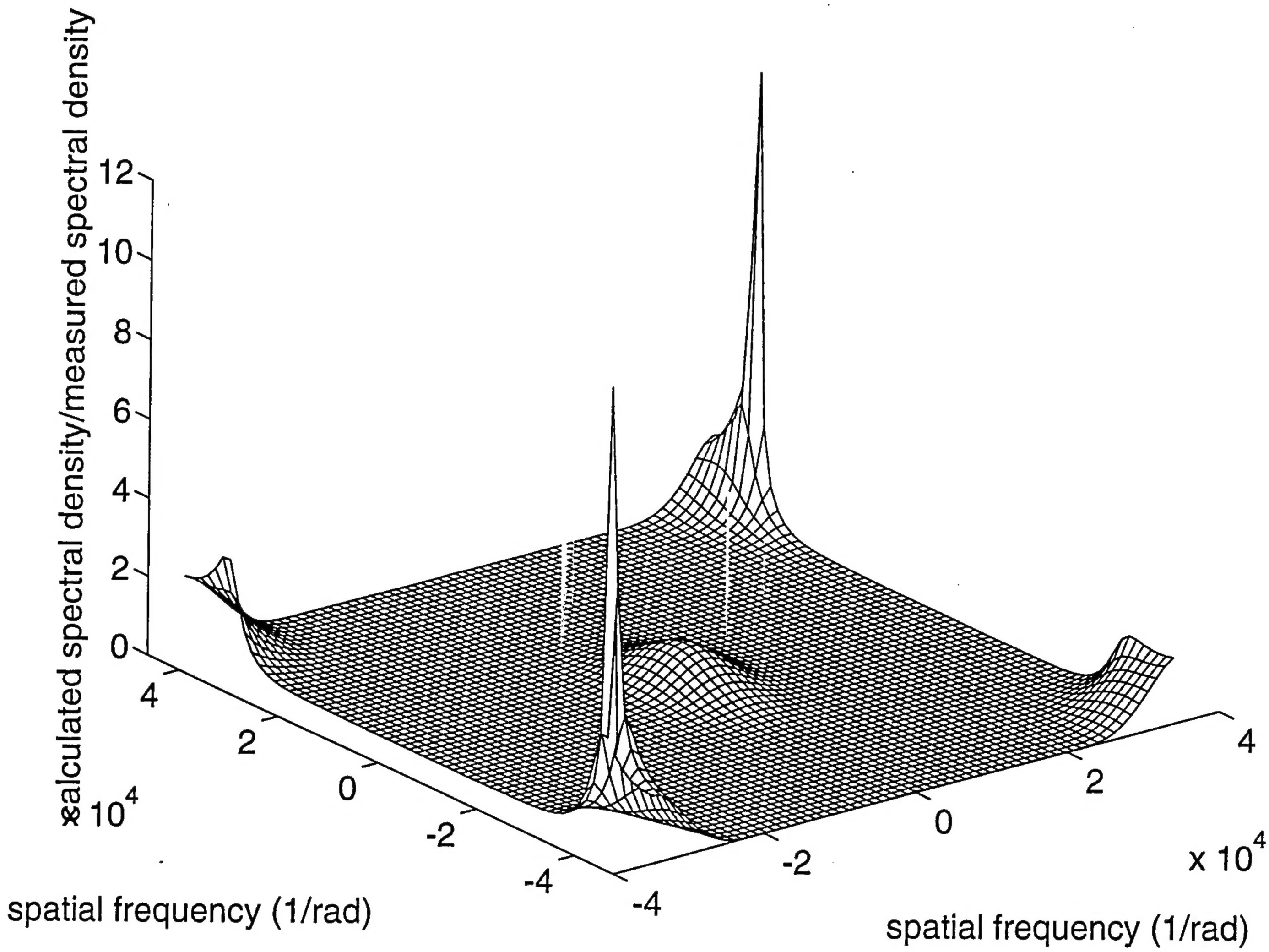

calculated spectral density/measured spectral density
12
10
8
6
4
2
0
4
2
0
-2
-4
x 10^4
spatial frequency (1/rad)
-4
-2
0
2
4
x 10^4
spatial frequency (1/rad)

Fig 5

original

restored

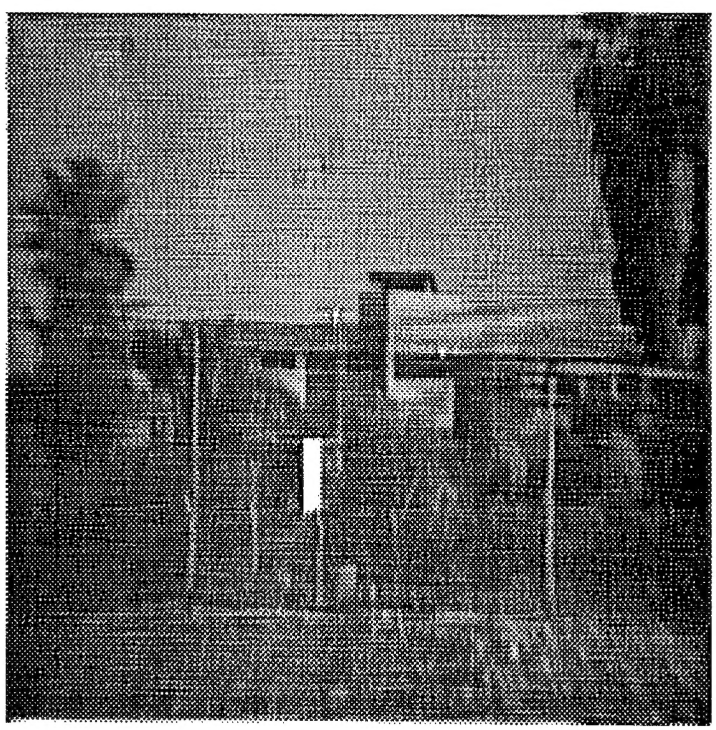

Fig. 6

original

restored

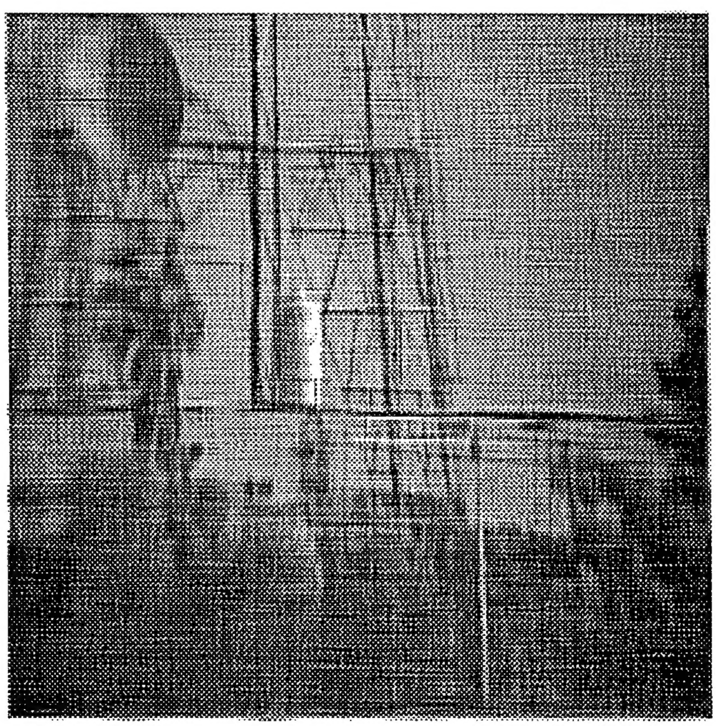

Fig. 7

original

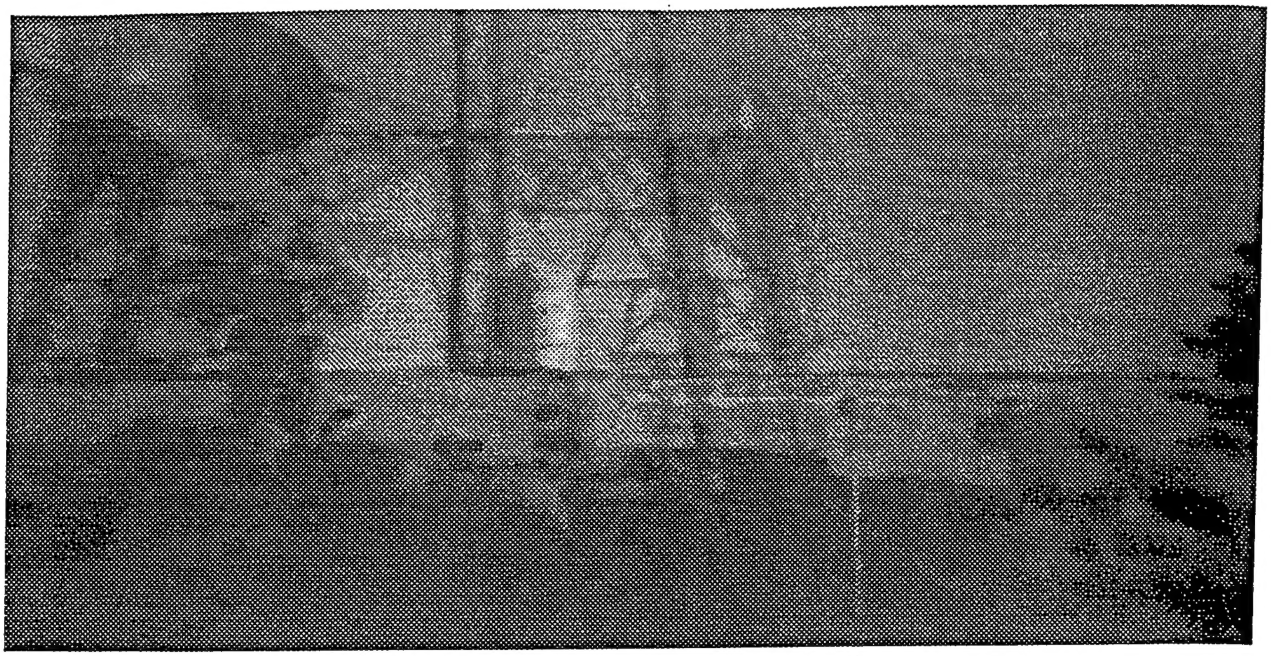

restored

Fig. 8